

# Phosphorus deficiencies invoke lipids-like enrich in sweetpotato rhizosphere to stimulate bacterial inositol phosphate metabolism

Xiaoya Zhu (✉ [1353040941@qq.com](mailto:1353040941@qq.com))

Xuzhou Sweetpotato Research Center

Jing Wang

Qiangqiang Zhang

Peng Zhao

Ming Liu

Rong Jin

Aijun Zhang

Zhonghou Tang

---

## Research Article

**Keywords:** Sweetpotato, rhizosphere, low P stress, bacterial community, metabolite profiles

**Posted Date:** July 5th, 2022

**DOI:** <https://doi.org/10.21203/rs.3.rs-1778928/v1>

**License:**  This work is licensed under a Creative Commons Attribution 4.0 International License.

[Read Full License](#)

---

# Abstract

*Purpose* Rhizosphere is the key part of belowground interaction between plant, microbes and soil. Beneficial interactions between plant roots and rhizosphere microorganisms are pivotal for plant fitness. Given the effort to improve sweetpotato phosphorus (P) efficiency, it is important to understand the adaptive strategies of sweetpotato rhizosphere under limited P availability. The aim of this study was to explore the variation of bacterial community and metabolite profiles of sweetpotato rhizosphere and their interactions under low P stress.

*Method* Rhizosphere samples collected from sweetpotato (Shangshu 19) grown in long-term (41 years) application nitrogen (N) and potassium (K) fertilizers (NK) and N, P and K fertilizers (NPK) soils were analyzed the bacterial community and metabolite profiles by 16S rRNA high-throughput sequencing and liquid chromatography-mass spectrometry (LC-MS), respectively.

*Conclusion* Different fertilization treatments significantly affected the abundances of rare genus in Shangshu 19 rhizosphere. The COG and KEGG enrichment analysis showed the function of bacterial correlated to sugar metabolism and inositol phosphate metabolism were significantly enhanced under low P stress. LC-MS analysis obtained similar results that galactose metabolism and phospholipase D signaling pathway were the top 2 differential metabolic pathways. Our results suggested that the bacteria of Shangshu 19 rhizosphere may use sugars as energy material to respond to low P stress by changing inositol phosphate metabolism. The increases of lipid-like substances played a connecting role, it was produced by sugar metabolism, and then entering mevalonate pathway activate inositol phosphate metabolism. These results have important practical significance for optimizing sweetpotato cultivation system.

## Introduction

Sweetpotato is one of the important food and economic crops in China, with a planting area of about 2 249 800 hectares and a total output of 49.2 million tons, accounting for 54.97% of the world's total output (FAO 2020). Phosphorus (P) is an essential element for plant growth and development, and plays an important role in crop yield increase (Jin et al. 2017). Numerous studies have shown that P availability is a key factor limiting the formation of sweetpotato yield and quality (Ryan et al. 2012; Gao et al. 2019). Insufficient P nutrition causes the decline of photosynthetic rate, abnormal carbon (C) and nitrogen (N) metabolism, and inhibition of carbohydrate accumulation and protein synthesis in sweetpotato (Kareem et al. 2020), which can lead to the loss of sweetpotato yield as high as 25%-60% (Villordon et al. 2020). For a long time, the application of P fertilizer is the most important means to increase soil P availability in actual agricultural production. However, P fertilizer is easy to be fixed by heavy metal ions and soil particles, or transformed into organic P ( $P_o$ ) that cannot be absorbed by plants, resulting in low utilization efficiency of P fertilizer in the current season, and plants will still suffer from low P stress (Ham et al. 2018). Some studies have pointed out that plant genotypes growing in low P fertility soil for a long time may have formed strategies to obtain and maintain nutrients by changing root structure (Nguyen and

stangoulis 2019), conservative distribution of P in plants (Ryan et al. 2012), changing exudation of root exudates (Minemba et al. 2020) and enrichment of microorganisms promoting plant growth (Gai et al. 2006). Therefore, exploring the feedback effect of sweetpotato to low P stress has important practical significance for optimizing sweetpotato cultivation system and realizing the synchronous improvement of P fertilizer utilization.

As an underground tuberous root crop, sweetpotato mainly absorbs phosphate through root interception (Lobet et al. 2019). Previous studies have shown that sweetpotato can absorb P to the maximum extent and increase yield to a certain extent by adjusting root structure (including root elongation, increase in the number and length of lateral roots and root hairs, etc.) under low P stress (Niu et al. 2013; López-Arredondo et al. 2014). Nevertheless, the rhizosphere is the gateway for various nutrients to enter the plant root system, and the rhizosphere environment directly affects the absorption and utilization of P by the root system. Recent studies have shown that sweetpotato obtained more P from low P soil mainly depends on the exudation of root organic acids and the reactivation of P by rhizosphere microorganisms, rather than on specialized root morphology (Minemba et al. 2019; Villordon et al. 2020). Additionally, plant root exudates can actively participate in the regulation of rhizosphere microbial activity and/or changes in quantity and community composition by changing the physical or chemical characteristics of the rhizosphere, thus affecting the process of rhizosphere nutrient cycling (Lebeis et al. 2015; Pang et al. 2021). For example, Zhang et al. (2018) found that root exudates can be rapidly utilized by mycelial microorganisms by using  $^{13}\text{C}$ -DNA-SIP tracing technology. At the same time, root exudates, as C source and signal material, stimulate the phosphate-solubilizing function of microorganisms and promote the activation of soil  $\text{P}_o$ . Unstable organic matter released from roots also accelerate the decomposition of soil organic matter (SOM) and stimulate rhizosphere microorganisms to dissolve insoluble minerals, thus promoting the release of N, P and other nutrients (Wang et al. 2016). However, the rhizodeposition of sweetpotato root exudate and its impacts on microbial community and on nutrient acquisition have received little attention to date, which is necessary to be further explored. If the rhizodeposition of sweetpotato root exudate can promote the activity and/or quantity of microorganisms beneficial to plant growth (such as N fixing bacteria, plant hormone producing bacteria and phosphate solubilizing bacteria, etc.) under low P stress, the impact of root exudates on microbial community will be particularly conducive to improving the yield of sweetpotato.

In this study, we analyzed the rhizosphere bacterial community and metabolites profiles of the low-P tolerant variety (Shangshu 19) growing in long-term (41 years) application of N and potassium (K) fertilizer (NK) and N, P and K fertilizer (NPK) soils by 16S rRNA high-throughput sequencing and liquid chromatography-mass spectrometry (LC-MS). The aims of this study were to identify the response characteristics and their interplay of bacterial community structure and metabolites profiles in the Shangshu 19 rhizosphere to low P stress. We hypothesized that: 1) low P stress would lead to the changes of bacterial community structure and metabolic spectrum in the rhizosphere of sweetpotato, and 2) the variations of metabolites in the rhizosphere were related to the changes of bacterial community.

# Materials And Methods

## General situation of test area

The test site is located in Jiangsu Xuzhou Sweet Potato Research Center (34°16' N, 117°17' E), Xuzhou City, Jiangsu Province. This area is a warm temperate semi humid climate zone, with an average annual temperature of 14 °C, and an average annual rainfall of 860 mm. Rainfall is mainly concentrated from July to August. The average annual evaporation is 1 870 mm, the annual frost-free period is about 210 days, and the sunshine hours are 2 317 hours. The long-term positioning test began in the autumn of 1980. The crop planting mode was wheat-maize rotation from 1981 to 2001, changed to wheat-sweet potato rotation after 2002. The variety of sweetpotato planted in 2021 was Shangshu 19. This variety was a low P tolerant variety, and also was the largest variety planted in China. Eight fertilization treatments were set in the experiment. Combined with the objectives of this study, three fertilizer application treatments were selected in this study, including 1) no fertilizer input (CK), 2) applied urea and diammonium phosphate (N, 150.0 kg hm<sup>-2</sup>) and potassium sulphate (K<sub>2</sub>O, 112.5 kg hm<sup>-2</sup>) (NK treatment), and 3) applied urea, calcium superphosphate (P<sub>2</sub>O<sub>5</sub>, 75.0 kg hm<sup>-2</sup>) and potassium sulphate (NPK treatment). The fertilizers were applied as the base fertilizer at one time. The physical and chemical properties of the original soil foundation were as follows: SOM content was 10.80 g kg<sup>-1</sup>, pH was 8.01, total N (TN) content was 0.66 g kg<sup>-1</sup>, total P (TP) content was 0.74 g kg<sup>-1</sup>, available P (AP) content was 12.00 mg kg<sup>-1</sup>, available K (AK) content was 63.00 mg kg<sup>-1</sup>, soil texture was sandy loamy. The survey of soil taxonomy was fluvo aquic soil, which was developed from yellow alluvial parent material.

## Sampling

Rhizosphere samples were collected after transplanting 110 days. During collection, ten sweetpotatoes were randomly selected under each fertilization treatment, and the rhizosphere soil was collected by “shaking off method” (Gao et al. 2019). After mixing evenly, they were used as one sample, and each treatment was repeated three times. Part of the collected soil was sieved and air dried for determining the basic soil chemical properties, and the other part was stored in a -80 °C refrigerator for high-throughput sequencing and determination of metabolome.

## Analysis of soil chemical properties

Soil SOM content was determined by the potassium dichromate oxidation external heating volumetric method (Nelson and Sommers 1982). Soil pH was measured in a suspension with a 1:2.5 soil to water ratio (w/v) and using an acidometer (Mettler Fe20, Shanghai). Soil TN content was determined by steam distillation after Kjeldahl digestion at 370°C (Zhu et al. 2020). Soil TP content was determined by HClO<sub>4</sub>-H<sub>2</sub>SO<sub>4</sub> digestion method followed by colorimetric spectrophotometry (Thomas et al. 1967). Soil AP content was extracted with 0.5 mol L<sup>-1</sup> NaHCO<sub>3</sub> (pH 8.5, soil to solution ratio 1:20) solution, and the extract was obtained by filtration. The P content in the extract was determined by molybdate colorimetry

(Olsen et al. 1954). Soil AK content was determined by  $1 \text{ mol L}^{-1} \text{ NH}_4\text{OAc}$  extraction followed by flame photometry.

### Analysis of soil bacterial diversity

Genomic DNA was extracted in duplicate from 0.10 g frozen soil using a PowerSoil® DNA Isolation Kit (MoBio, Carlsbad, CA, USA) following the manufacturer's instructions. The DNA concentration and quality were assessed by the A260/280 and A260/230 ratios using a NanoDrop ND-2000 spectrophotometer (Thermo Scientific Wilmington, DE, USA). The isolated DNA was stored at  $-80^\circ\text{C}$  for further analysis. Using the extracted DNA sample as a template, the bacterial 16S rRNA V3-V4 region was amplified with primer 338F: 5'-ACTCCTACGGGAGGCAGCA-3', 806R: 5'-GGACTACHVGGGTWTCTAAT-3'. PCR reaction systems were all 25  $\mu\text{L}$ , including DNA sample 3  $\mu\text{L}$ , each primer 1  $\mu\text{L}$ , and nuclease free water 20  $\mu\text{L}$ . PCR reaction conditions were as follows:  $94^\circ\text{C}$  for 5 min; followed by 30 cycles at  $94^\circ\text{C}$  for 30 s,  $52^\circ\text{C}$  for 30 s, and  $72^\circ\text{C}$  for 30 s; and a final extension at  $72^\circ\text{C}$  for 10 min. The fragment length and concentration of PCR products were detected by 1% agarose gel electrophoresis. After the concentration of PCR products was compared by GeneTools analysis software (Version 4.03.05.0, SynGene), the required volume of each sample was calculated according to the principle of equal mass, and the PCR products were mixed. Using E.Z.N.A.® Gel Extraction Kit recovered PCR mixed products, and TE buffer eluted and recovered target DNA fragments. As per NEBNext® Ultra™ DNA Library Prep Kit for Illumina standard process for building database. The constructed sequencing library was inspected, and the qualified library was sequenced with Illumina HiSeq PE250. Trimmatic software (V0.33) was used to filter the quality of two terminal raw reads data respectively to obtain the paired-end clean reads after quality control. According to the barcode and primer information at the beginning and end of the sequence, the barcode and primer were removed by using Mathur software (V1.35.1), and finally effective splice fragments (Clean Tags) were obtained. Using USEARCH software (V10) to cluster all clean tags of all samples. By default, the sequences were clustered into operational taxonomic units (OTUs) with 97% consistency. One OTU represented one species. The default clustering method was UPARSE. At the same time, the sequence with the highest frequency will be used as the representative sequence of each OTU for subsequent annotation. Using assign\_taxonomy.py script in QIIME software will compare the representative sequence of each OTU after removing chimera and Singleton with Silva database to obtain species annotation information. Take the sample with the least number of sequences as the standard, normalize all samples for subsequent analysis.

### Analysis the metabolic profiling of rhizosphere soil

Soil sample was weighed 0.50 g, and then added 20  $\mu\text{L}$  internal standard (L-2-chlorophenylalanine, 0.06 mg/mL, methanol configuration) and 1 mL of methanol water (V: V = 1:1). Two small steel balls were added successively, and put them into a grinder for grinding (60 Hz, 2 min) after precooling at  $-20^\circ\text{C}$  for 2 min. The homogenized sample was transferred to a 15 mL centrifuge tube, and was centrifuged for 10 min (7700 rpm,  $4^\circ\text{C}$ ). 2.5 mL supernatant was taken into a 5 mL centrifuge tube and freeze dry. The 400  $\mu\text{L}$  methanol water (V: V = 1:4) was used for dissolving freeze-dried sample, and then vortex oscillation for

60 s, ultrasonic for 30 s, centrifugation for 10 min (12000 rpm, 4 °C). 150 µL supernatant was sucked with a syringe, and then transferred to LC injection vial and stored at -80 °C after using 0.22 µm organic phase pinhole filter. LC-MS analysis was performed using the following conditions: the chromatographic column used ACQUITY UPLC HSS T3 (100 mm×2.1 mm, 1.8 µm), column temperature: 45 °C, mobile phase: A-water (containing 0.1% formic acid), B-acetonitrile (containing 0.1% formic acid), flow rate: 0.35 mL/min, injection volume: 2 µL. The mass spectrum condition was ESI ion source. The sample mass spectrum signals were collected by positive and negative ion scanning mode.

## Data statistics and analysis

Venn diagram was used to count the number of common and unique OTUs among different treatments. One-way ANOVA was performed using IBM SPSS Statistics 22.0 (IBM, USA). In order to more intuitively showed the expression differences of metabolites between different treatments, the volcanic plot was used to visualize the *P*-value and Log<sub>2</sub> (Fold Change) value and screen the differential expressed metabolites (DEMs). Biological pathway analysis was performed based on 16s rRNA and LC-MS data using MetaboAnalyst 4.0. Heatmaps displayed differential genus and the DEMs between different treatments. Redundancy analysis (RDA) was used to evaluate the effect of environmental factors on the distribution characteristics of bacterial community of Shangshu 19 rhizosphere (Canoco 5.0). The network diagram was used to show the correlations between microorganisms and DEMs. Both heatmaps and network diagram were carried out on the cloud platform of Ouyi company (Shanghai, China).

## Results

### Soil chemical properties

Compared with CK treatment, long-term fertilization (NK and NPK) significantly increased the contents of soil SOM, TN, AP and AK, especially in NPK treatment (Table 1), the contents of soil SOM, TN and AP increased by 31.8%, 54.5% and 81.3%, respectively ( $P < 0.05$ ), while soil pH and NH<sub>4</sub><sup>+</sup>-N content decreased significantly ( $P < 0.05$ ). There was no significant difference in soil TP content between CK and NK treatments, which were significantly lower than that of NPK treatment ( $P < 0.05$ ). The contents of NO<sub>3</sub><sup>-</sup>-N and AK were the highest in NK treatment, which were 41.2% and 84.3% higher than those in NPK treatment, respectively ( $P < 0.05$ ).

Table 1  
Soil chemical properties of different fertilization treatments

Treatment	SOM (g kg <sup>-1</sup> )	pH	TN (g kg <sup>-1</sup> )	TP (g kg <sup>-1</sup> )	NH <sub>4</sub> <sup>+</sup> -N (mg kg <sup>-1</sup> )	NO <sub>3</sub> <sup>-</sup> -N (mg kg <sup>-1</sup> )	AP (mg kg <sup>-1</sup> )	AK (mg kg <sup>-1</sup> )
CK	12.25 ± 0.28 c	8.70 ± 0.02 a	0.77 ± 0.07 c	0.78 ± 0.04 b	0.88 ± 0.13 a	3.74 ± 0.41 c	4.80 ± 0.37 c	52.25 ± 3.30 c
NK	12.85 ± 0.32 b	8.46 ± 0.05 b	0.94 ± 0.05 b	0.72 ± 0.03 b	0.48 ± 0.10 b	7.44 ± 0.31 a	5.28 ± 0.77 b	138.25 ± 0.96 a
NPK	16.15 ± 0.16 a	8.40 ± 0.01 c	1.19 ± 0.19 a	1.14 ± 0.08 a	0.13 ± 0.05 c	5.27 ± 0.22 b	8.70 ± 0.97 a	75.00 ± 0.82 b

\*The data in the table are mean ± standard deviation (n = 3). Different letters in the same column indicate significant differences (P < 0.05)

### Microbial community of rhizosphere

Based on the results of high-throughput sequencing of 16S rRNA, a total of 15 213 bacterial OTUs were identified in Shangshu 19 rhizosphere, and 5 146 OTUs were shared among different treatments (Fig. 1A). Compared with CK treatment, the number of OTUs of Shangshu 19 rhizosphere in NK and NPK treatments decreased by 35.1% and 22.7%, respectively. Indicating that long-term fertilization will reduce the bacterial OTUs number of Shangshu 19 rhizosphere. The number of OTUs of Shangshu 19 rhizosphere in NK treatment were 15.9% lower than that of NPK treatment (P < 0.05). The OTUs detected in this study can be further divided into 11 phyla, 13 classes, 23 orders, 21 families and 14 genera (relative abundance > 1%). Proteobacteria, Gemmatimonadota, Bacteroidota and Actinobacteriota were the dominant phylum, accounting for 74.7%-76.3% (Fig. S1). At the genus level, *MND1* (5.5%-6.1%), *Sphingomonas* (4.1%-5.0%), *TRA3-20* (2.1%-2.4%) and *Nitrospira* (1.9%-2.2%) were the dominant genera (Fig. 1B). Different fertilization treatments had no significant effect on the relative abundance of top15 bacterial genera (P > 0.05), but there were significant differences in the relative abundance of some rare genera among different treatments (Fig. 1C). Compared with CK treatment, the relative abundances of *Bacillus* and *Ellin6067* of Shangshu 19 rhizosphere decreased significantly in NK and NPK treatments (P < 0.05), and the relative abundances of *Acidibacter* decreased significantly without long-term application of phosphate fertilizer (NK), while that increased significantly with long-term application of phosphate fertilizer (NPK) (P < 0.05). Compared with NPK treatment, the relative abundances of *Bacillus*, *Azoarcus* and *IMCC26256* of Shangshu 19 rhizosphere in NK treatment were significantly increased by 150.5%, 615.2% and 78.0%, respectively (P < 0.05), and the relative abundances of *OM27\_clade*, *Acidibacter*, *Polyclovorans* and *Bryobacter* decreased significantly (P < 0.05). According to the results of heatmap clustering, the rhizosphere bacterial communities between CK and NK treatments were similar, and they were different from NPK treatment, but there was no significant difference in α-diversity among three treatments (P < 0.05) (Fig. 1D).

The prediction results of COG and KEGG based on 16s rRNA sequences were shown in Fig. 2. The predicted homologous protein clusters reached 4 445, of which 237 were significantly different ( $P < 0.05$ ). Among them, the top 10 COGs of functional prediction was mainly related to metabolism, including four Carbohydrate transport and metabolism (ABC-type sugar transport system, ATPase component; Ribose/xylose/arabinose/galactoside ABC-type transport systems, permease components; ABC-type sugar transport systems, permease components; Alpha-L-arabinofuranosidase), two Energy production and conversion (Coenzyme F420-reducing hydrogenase, beta subunit; Phosphoenolpyruvate carboxykinase), one amino acid transport and metabolism (Acetolactate synthase), one Cell wall/membrane/envelope biogenesis (D-alanyl-D-alanine carboxypeptidase) and one Secondary metabolites biosynthesis, transport, and catabolism (Cyanophycinase and related exopeptidases), their relative abundances in NK treatment were significantly higher than those in CK and NPK treatments (Fig. 2A). Among them, Carbohydrate transport and metabolism were mainly related to sugar metabolism. The results of KEGG function prediction showed that there were significant differences in 10 metabolic pathways at KEGG\_L3 level ( $P < 0.05$ ). Among them, the relative abundance of Inositol phosphate metabolism and Transporters in NK treatment was significantly higher than that in NPK treatment (Fig. 2B).

### Metabolic profiling of rhizosphere

Based on the results of LC-MS analysis, 4 511 kinds of DEMs were identified, including 1 710 unclassified metabolites. The remaining DEMs were mainly Lipids and lipid like molecules (1 155), followed by Organic acids and derivatives (401). The metabolites were screened according to  $VIP > 1$  and  $P < 0.05$ , and there were 35 DEMs between NK and NPK treatments (Fig. 3A). These DEMs were mainly Lipids and lipid like molecules (13) and Organooxygen compounds (9), followed by Organic acids and derivatives (4) (Fig. 3B). Compared with NPK treatment, 12 DEMs were significantly up-regulated and 23 DEMs were significantly down-regulated in NK treatment ( $P < 0.05$ ). Specifically, the expression of Organic compounds and Organic acids and derivatives decreased significantly in NK treatment, while 8 of the 12 metabolites with significantly increased expression were Lipids and lipid like molecules ( $P < 0.05$ ), including Eplerenone, (3Z, 6Z)-3, 6-Nonadien-1-ol, Ganoderal A, 9-B1-PhytoP, MG (18:1 (9Z) /0:0/0:0) [rac], Petasalbin, Prenyl glucoside and (2xi, 6xi) -7-Methyl-3-methylene-1, 2, 6, 7-octanetetroleplerenone (Fig. S2). According to the results of KEGG enrichment analysis, 36 differential metabolic pathways were enriched in Shangshu 19 rhizosphere. Among them, the Galactose metabolism pathway had a very significant difference among different treatments ( $P < 0.001$ ), followed by Phospholipase D signaling pathway ( $P = 0.011$ ), D-Glutamine and D-glutamate metabolism ( $P = 0.013$ ) (Fig. 3C). DEMs involved in 36 differential metabolic pathways included L-Glutamate, Galactonic acid, D-Gal alpha 1->6D-Gal alpha 1->6D-Glucose, Alpha-Linolenic acid and Mevalonate-P (Fig. S3), and their expression levels were lower in NK treatment than NPK treatment ( $P < 0.05$ ). Among them, the expression of phosphate monoesters (Mevalonate-P) decreased the most (decreased by 71.0%).

### Correlation analysis of environmental factors and soil bacterial community

The results of RDA analysis showed that the rhizosphere bacterial community of Shangshu 19 were separated according to different fertilization treatments (Fig. 4). RDA1 axis and RDA2 axis explained 73.6% and 21.2% of the total variation of bacterial community structure, respectively. The conditional effect analysis showed that the contents of soil AK and  $\text{NO}_3^-$ -N were the main factors affecting the distribution of bacterial community in the rhizosphere of Shangshu 19, explaining 38.8% and 34.7% of the variation of bacterial community structure, respectively ( $P < 0.05$ ). RDA1 axis was mainly related to the contents of  $\text{NO}_3^-$ -N and AK. RDA2 axis was greatly affected by  $\text{NH}_4^-$ -N. The rhizosphere bacterial communities of NK and NPK treatments were mainly separated from each other along the RDA1 axis, but they were similar on the RDA2 axis. They were separated from each other that of CK treatment along the RDA2 axis. The relative abundances of *Bacillus*, *Azoarcus* and *IMCC26256* were significantly positively correlated with AK and  $\text{NO}_3^-$ -N contents, and negatively correlated with AP content ( $P < 0.05$ ). The relative abundances of *OM27\_Clade*, *Acidibacter*, *Polyclovorans* and *Bryobacter*, on the contrary, showed a significant negative correlation with soil  $\text{NO}_3^-$ -N content and a significant positive correlation with AP content ( $P < 0.05$ ). The relative abundance of *Alterythrobacter* was positively correlated with soil available nutrients ( $\text{NO}_3^-$ -N, AP, AK) ( $P < 0.05$ ).

As shown in Fig. 5, the positive correlations between the bacteria genus with DEMs were more than the negative correlations. Among them, *IMCC26256*, *Polyclovorans*, *Bryobacter* and DEMs had the most connections. Specifically, the negative correlations between *IMCC26256* and DEMs was more than the positive correlations, and it only positively correlated to (3Z, 6Z)-3, 6-Nonadien-1-ol, Ganoderol A and N, N, O-Tridesmethyltramadol. The correlation coefficients were 0.94, 0.86 and 0.88, respectively ( $P < 0.05$ ). *Azoarcus* was also had positive correlations with (3Z, 6Z)-3, 6-Nonadien-1-ol ( $r = 0.94$ ,  $P = 0.02$ ) and N, N, O-Tridesmethyltramadol ( $r = 0.99$ ,  $P < 0.001$ ), respectively. They were all negatively correlated with the expression of mevalonate-P ( $P < 0.05$ ). *Bacillus* was only positively correlated to (2xi, 6xi) -7-methyl-3-methyl-1, 2, 6, 7-octanetrol ( $r = 0.86$ ,  $P = 0.03$ ).

## Discussion

### Changes and causes of the bacterial community structure of Shangshu 19 rhizosphere

Rhizosphere is the hub of material, energy flow and information exchange in plant-soil ecosystem, and is considered to be the key area of nutrient cycle (Fabianska et al. 2019). There are a large number of microorganisms in the rhizosphere, which can use their own metabolic functions to drive the rhizosphere soil nutrient cycle and directly affect the soil nutrient turnover and supply level (Zhalnina et al. 2018). Our results showed that the application of P fertilizer or not changed the relative abundance of rare genus in Shangshu 19 rhizosphere, indicating that they played an important role in responding to the soil P level. The relative abundances of *Bacillus*, *Azoarcus* and *IMCC26256* of Shangshu 19 rhizosphere in the long-term no P fertilizer (NK) treatment were significantly higher than those in the NPK treatment (Fig. 1C), which played an important role in the soil N cycle, including biological N fixation and nitrification (Jorquera et al. 2011; Sui et al. 2020). The results of soil  $\text{NH}_4^+$ -N and  $\text{NO}_3^-$ -N contents in NK treatment

were higher than that of in NPK treatment (Table 1) supported this point. Generally speaking, the growth of microorganisms must maintain a stable N/P ratio. On the one hand, increasing N input will increase the demand of microorganisms for inorganic P ( $P_i$ ), promote the assimilation of P by soil microorganisms, and enhance the ability of microorganisms to dissolve  $P_i$  and mineralize  $P_o$ , so as to obtain more  $P_i$  for microbial growth (Xiao et al. 2018). For example, most results from natural forests, short-term field trials or pot experiments showed that N input contributes to microbial P fixation under low P conditions (Spohn et al. 2018). In addition, many studies have shown that nitrate signal can trigger the regulation of plant phosphate starvation response, such as improve the activity of soil phosphatase or increase the expression of gene abundance involved in  $P_i$  dissolution and  $P_o$  mineralization (Deng et al. 2016; Dai et al. 2020). Jorquera et al. (2010) reported that *Bacillus* encoded phytase (*BPP*) gene, which had the function of mineralizing inositol phosphate. This study also obtained consistent results. KEGG enrichment analysis of 16S rRNA gene sequencing results showed that the relative abundance of inositol phosphate metabolism in NK treatment was significantly higher than that in NPK treatment (Fig. 2B). This may be one of the reasons why the soil AP content of NK treatment was higher than that of CK treatment (Table 1). Soil AP content of NPK treatment was naturally higher due to the input of P fertilizer (Table 1). The result of soil AP content in NK treatment was significantly lower than that in NPK treatment also suggested that although the functional potential of P receptors was enhanced due to N fertilizer input, the functional potential of genes involved in P absorption and transport and the P assimilation process of corresponding microorganisms were still limited. The COG analysis results based on 16S rDNA gene sequencing results showed that the rhizosphere microorganisms of Shangshu 19 were mainly related to sugar metabolism (Fig. 2A), because the microorganisms need to use C sources to provide energy in the process of maintaining nutritional homeostasis (Paul 2014).

The results of RDA analysis showed that the content of soil AK was the primary factor leading to the change of bacterial community structure of Shangshu 19 rhizosphere between different fertilization treatments (Fig. 4), followed by the content of soil  $\text{NO}_3^-$ -N, which may be related to the fact that sweetpotato is a K-loving crop (Tanaka 2016). Previous studies have shown that soil pH was the main factor affecting the microbial community structure of grassland, forest and arable (Wang et al. 2012; Ragot et al. 2015). This study did not get the same results. Although the long-term application of N fertilizer (NK and NPK treatment) significantly reduced the soil pH (Table 1), the impact of long-term N input on the microbial community was less than the N effect itself (i.e., the stoichiometric ratio of N and P). It is worth noting that long-term low P conditions (i.e., no P input for many years) may lead to irreversible changes in the microbial community, leading to the transformation of  $P_o$  mineralized microorganisms into relatively inactive and dormant states (Gyaneshwar et al. 2002). As shown in the results of this study, the dominant soil bacteria such as *MND1* and *Nitrospira* in different fertilization treatments were also related to the N cycle (Fig. 2B), and their relative abundance did not change with the input of P fertilizer.

Changes and causes of the metabolite profiles of Shangshu 19 rhizosphere

Root systems rapidly extended their functionality and complexity with the domestication and improvement of plants from natural ecosystems to modern agriculture (Kenrick and Strullu-Derrien, 2014). Plant roots showed strong developmental plasticity through their secretory activities, including low-molecular-weight compounds (such as phenolics, amino acids, nucleotides, sugars, terpenoids, and lipids) and high-molecular-weight compounds (such as nucleic acids, polysaccharides, and proteins), enable it to respond to various environmental conditions (Berendsen et al. 2012). The types of compounds and their relative abundances depend on the species of plants, their growth and developmental stages, and presence of stress (abiotic, biotic) factors (Korenblum et al. 2020). The research showed that plant-derived flavones enrich in rhizosphere improving maize performance under N deprivation (Yu et al. 2021), and coumarins contribute to the developing of *Arabidopsis* under iron deficiency (Voges et al. 2019).

In this study, KEGG enrichment analysis of detected DEMs showed that the expression of Mevalonate-P in rhizosphere decreased the most in NK treatment (Fig. S3), while the expression of sesquiterpenoids (Petasalbin) and triterpenoids (Ganoderal A) substances related to this substance increased significantly. They were the intermediates and metabolites of mevalonate pathway, respectively. Indicating that low P stress promoted the progress of mevalonate pathway. This was demonstrated by the KEGG enriched differential metabolic pathway terpenoid backbone biosynthesis ( $P < 0.05$ ) (Fig. 3C). Galactose metabolism and phospholipase D signaling pathway were the top 2 differential metabolic pathways detected by KEGG enrichment analysis (Fig. 3C), which was consistent with the correlations between rhizosphere bacterial function and sugar metabolism and inositol phosphate metabolism predicted based on COG and KEGG analysis (Fig. 2A). Because the raw material of mevalonate pathway was Acetyl CoA produced by glycolysis pathway (Chappell 1995). The results of Helletsgruber et al. (2017) showed that bacteria belonging to the genera *Bacillus* and *Sphingomonas* could exploit certain plant volatile organic compounds (i.e., terpenoid) as C source. Phospholipase D signaling pathway was the result of synergistic effect of phosphatidylinositol and  $\text{Ca}^{2+}$  or stimulation of unsaturated fatty acids (Zheng et al. 2000), which to some extent explained that up-regulated DEMs contained more kinds of unsaturated fatty acids. These results showed that the rhizosphere microorganisms of Shangshu 19 used sugars as energy materials to respond to low P stress by changing inositol phosphate metabolism. But the mechanism needs further study.

The rhizosphere deposition of root exudates mediates the influence of microbial community on plant nutrition, especially under the condition of nutritional stress, which plays an irreplaceable role in alleviating environmental stress and activating soil nutrients. There was growing evidence that plants can release up to 20%-40% of their photo assimilate-derived C via their roots as exudates (Wang et al. 2021). They either change the chemical properties of rhizosphere and change the living environment of soil microorganisms (Ren et al. 2021), or act as a medium for microbial growth (Rogers et al. 2020) so as to change the rhizosphere microbial community and affect the nutrient cycle process. Recent findings demonstrated that specific metabolites such as benzoxazinoids (Cotton et al. 2019), salicylic acid (Kong et al. 2020), siderophore (Sun et al. 2019) and flavones (Yu et al. 2021) in plants have been demonstrated

to confer root-type-specific changes of microbial community to response nutrient stress. Our results showed that the accumulation of lipids-like substances including (3Z, 6Z)-3, 6-Nonadien-1-ol, Ganoderal A, Petasalbin and (2xi, 6xi) -7-Methyl-3-methylene-1, 2, 6, 7-octanetetrol in rhizosphere promoted the enrichment of bacteria correlated to N cycling (i.e., *IMCC26256*, *Azoarcus* and *Bacillus*) under low P stress. This was consistent with the previous research results. That was, the condition of sufficient N and lack of P may stimulate microbial N metabolism and promote the release of P in organic N and P compounds to maintain nutrient balance (Lu et al. 2020). This was also supported by the differential expression of D-Glutamine and D-glutamate metabolism and nitrogen metabolism pathways that were enriched by KEGG analysis (Fig. 3C). Based on the above results, future studies need to unravel the complexity of root microbial interaction mediated by host derived metabolites and the molecular mechanism of this interaction.

## Conclusions

The relative abundances of dominant genus *MND1*, *Sphingomonas* and *Nitrospira* (abundance > 1%) in Shangshu 19 rhizosphere had no significant change under long-term no P fertilizer application (NK treatment) ( $P > 0.05$ ). However, the relative abundances of rare genus *IMCC26256*, *Azoarcus* and *Bacillus* increased significantly ( $P < 0.05$ ). Based on the enrichment analysis of COG and KEGG, the sugar metabolism and inositol phosphate metabolism function of bacteria in Shangshu 19 rhizosphere were significantly enhanced ( $P < 0.05$ ). The same results were obtained by KEGG analysis of the metabolism profiles of Shangshu 19 rhizosphere by LC-MS. Galactose metabolism and phospholipase D signaling pathway were the top 2 differential metabolic pathways ( $P < 0.05$ ). These results showed that the microorganisms of Shangshu 19 rhizosphere used sugars as energy materials to respond to low P stress by changing inositol phosphate metabolism. This may be related to the significant increase in the expression of lipids-like substances in Shangshu 19 rhizosphere.

## Declarations

**Declaration of competing interest** The authors declare that they have no conflict of interest.

**Acknowledgements** This work was supported the National Natural Science Foundation of China (31771721) and the Provincial Key R&D Program of Jiangsu [BE2021311].

## References

1. Berendsen RL, Pieterse CMJ, Bakker PAHM (2012) The rhizosphere microbiome and plant health. Trends Plant Sci 17:478–486. <http://doi.org/10.1016/j.tplants.2012.04.001>
2. Chappell J (1995) Biochemistry and molecular biology of the isoprenoid biosynthetic pathway in plants. Annu Rev Plant Physiol Plant Mol Biol 46:521–547. <http://doi.org/10.1146/annurev.pp.46.060195.002513>

3. Cotton TEA, Pétriacq P, Cameron DD, Meselmani MA, Schwarzenbacher RE, Rolfe SA, Ton J (2019) Metabolic regulation of the maize rhizobiome by benzoxazinoids. *ISME J* 13:1647–1658. <http://doi.org/10.1038/s41396-019-0375-2>
4. Dai ZM, Liu GF, Chen HH, Chen CG, Wang JK, Ai SY, Wei D, Li DM, Ma B, Tang CX, Brookes PC, Xu JM (2020) Long-term nutrient inputs shift soil microbial functional profiles of phosphorus cycling in diverse agroecosystems. *ISME J* 14:757–770. <https://doi.org/10.1038/s41396-019-0567-9>
5. Deng M, Liu L, Sun Z, Piao S, Ma Y, Chen Y, Wang J, Qiao C, Wang X, Li P (2016) Increased phosphate uptake but not resorption alleviates phosphorus deficiency induced by nitrogen deposition in temperate *Larix principis-rupprechtii* plantations. *New Phytol* 212:1019–1029. <https://doi.org/10.1111/nph.14083>
6. Fabianska I, Gerlach N, Almario J, Bucher M (2019) Plant-mediated effects of soil phosphorus on the root-associated fungal microbiota in *Arabidopsis thaliana*. *New Phytol* 221:2123–2137. <https://doi.org/10.1111/nph.15538>
7. FAO Database. [DB/OL] (2020) -2-6). [2022-2-15] <https://www.fao.org/faostat/zh/#faq>
8. Gai JP, Feng G, Christie P, Li XL (2006) Screening of arbuscular mycorrhizal fungi for symbiotic efficiency with sweet potato. *J Plant Nutr* 29:1085–1094. <https://doi.org/10.1080/01904160600689225>
9. Gao P, Liu Y, Wang Y, Liu X, Wang Z, Ma LQ (2019) Spatial and temporal changes of P and Ca distribution and fractionation in soil and sediment in a karst farmland-wetland system. *Chemosphere* 220:644–650. <http://doi.org/10.1016/j.chemosphere.2018.12.183>
10. Gyaneshwar P, Kumar GN, Parekh LJ, Poole PS (2002) Role of soil microorganisms in improving P nutrition of plants. *Syst Sci Compr Stud Agric* 245:133–143. <http://doi.org/10.1023/A:1020663916259>
11. Ham BK, Chen J, Yan Y, Lucas WJ (2018) Insights into plant phosphate sensing and signaling. *Curr Opin Biotechnol* 49:1–9. <http://doi.org/10.1016/j.copbio.2017.07.005>
12. Helletsgruber C, Dötterl S, Ruprecht U, Junker RR (2017) Epiphytic bacteria alter floral scent emissions. *J Chem Ecol* 43:1073–1077. <http://doi.org/10.1007/s10886-017-0898-9>
13. Lu JY, Yang JF, Keitel C, Yin LM, Wang P, Cheng WX, Dijkstra FA (2020) Rhizosphere priming effects of *Lolium perenne* and *Trifolium repens* depend on phosphorus fertilization and biological nitrogen fixation. *Soil Biol Biochem* 150:108005. <http://doi.org/10.1016/j.soilbio.2020.108005>
14. Jin KM, White PJ, Whalley WR, Shen J, Shi L (2017) Shaping an optimal soil by root-soil interaction. *Trends Plant Sci* 22(10):823–829. <http://doi.org/10.1016/j.tplants.2017.07.008>
15. Jorquera MA, Crowley DE, Marschner P, Greiner R, Fernández MT, Romero D, Blackburn DM, De La Luz Mora M(2011) Identification of  $\beta$ -propeller phytase-encoding genes in culturable *Paenibacillus* and *Bacillus spp.* from the rhizosphere of pasture plants on volcanic soils. *FEMS Microbiol Ecol* 75(1):163–172. <http://doi.org/10.1111/j.1574-6941.2010.00995.x>
16. Kareem I, Akinrinde EA, Oladosu Y, Eifediyi EK, Adekola OF (2020) Enhancement of phosphorus uptake, growth and yield of sweet potato (*Ipomoea batatas*) with phosphorus fertilizers. *J Appl Sci*

- Environ Manage 24(1):79–83. <http://doi.org/10.4314/jasem.v24i1.11>
17. Kenrick P, Strullu-Derrien C (2014) The origin and early evolution of roots. *Plant Physiol* 166:570–580. <http://doi.org/10.1104/pp.114.244517>
  18. Kong HG, Song GC, Sim HJ, Ryu CM (2020) Achieving similar root microbiota composition in neighbouring plants through airborne signalling. *ISME J* 15:397–408. <http://doi.org/10.1038/s41396-020-00759-z>
  19. Korenblum E, Dong Y, Szymanski J, Panda S, Jozwiak A, Massalha H, Meir S, Rogachev I, Aharoni A (2020) Rhizosphere microbiome mediates systemic root metabolite exudation by root-to-root signaling. *Proc Natl Acad Sci USA* 117:3874–3883. <http://doi.org/10.1073/pnas.1912130117>
  20. Lebeis SL, Paredes SH, Lundberg DS, Breakfield N, Gehring J, McDonald M, Malfatti S, Glavina del Rio TG, Jones CD, Tringe SG, Dangl JL (2015) Plant microbiome. Salicylic acid modulates colonization of the root microbiome by specific bacterial taxa. *Science* 349:860–864. <http://doi.org/10.1126/science.aaa8764>
  21. Lobet G, Paez-Garcia A, Schneider H, Junker A, Atkinson JA, Tracy S (2019) Demystifying roots: A need for clarification and extended concepts in root phenotyping. *Plant Sci* 282:11–13. <http://doi.org/10.1016/j.plantsci.2018.09.015>
  22. López-Arredondo DL, Leyva-González MA, González-Morales SI, López-Bucio J, Herrera-Estrella L (2014) Phosphate nutrition: improving low-phosphate tolerance in crops. *Annu Rev Plant Biol* 65:95–123. <http://doi.org/10.1146/annurev-arplant-050213-035949>
  23. Minemba D, Gleeson DB, Veneklaas E, Ryan MH (2019) Variation in morphological and physiological root traits and organic acid exudation of three sweet potato (*Ipomoea batatas*) cultivars under seven phosphorus levels. *HortScience: a publication of the American Society for Horticultural Science* 256:108572. <http://doi.org/10.1016/j.scienta.2019.108572>
  24. Nelson DW, Sommers LE(1982) Total carbon, organic carbon and organic matter. In: *Methods of soil analysis*. Amer Soc Agron 539–579
  25. Niu YF, Chai RS, Jin GL, Wang H, Tang CX, Zhang YS (2013) Responses of root architecture development to low phosphorus availability: A review. *Ann Bot* 112:391–408. <http://doi.org/10.1093/aob/mcs285>
  26. Nguyen VL, Stangoulis J (2019) Variation in root system architecture and morphology of two wheat genotypes is a predictor of their tolerance to phosphorus deficiency. *Acta Physiol Plant* 4:109. <http://doi.org/10.1007/s11738-019-2891-0>
  27. Olsen SR, Cole CV, Watanabe FS, Dean LA (1954) Estimation of available phosphorus in soils by extraction with sodium bicarbonate. United States Department of Agriculture Circular No. 939
  28. Pang ZQ, Chen J, Wang TH, Gao CS, Li ZM, Guo LT, Xu JP, Cheng Y (2021) Linking plant secondary metabolites and plant microbiomes: A Review. *Front Plant Sci* 12:621276. <http://doi.org/10.3389/fpls.2021.621276>
  29. Paul EA (2014) *Soil microbiology, ecology and biochemistry*, 4th edn. NW1, UK: Academic press, London

30. Ragot SA, Kertesz MA, Bunemann EK (2015) *phoD* alkaline phosphatase gene diversity in soil. *Appl Environ Microb* 81(20):7281–7289. <http://doi.org/10.1128/AEM.01823-15>
31. Ren X, Tang J, Wang L, Liu Q (2021) Microplastics in soil-plant system: effects of nano/microplastics on plant photosynthesis, rhizosphere microbes and soil properties in soil with different residues. *Plant Soil* 462:561–576. <https://doi.org/10.1007/s11104-021-04869-1>
32. Rogers KL, Carreres-Calabuig JA, Gorokhova E, Posth NR (2020) Micro-by-micro interactions: how microorganisms influence the fate of marine microplastics. *Limnol Oceanogr Lett* 5:18–36. <https://doi.org/10.1002/lol2.10136>
33. Ryan MH, Tibbett M, Edmonds-Tibbett T, Suriyagoda LDB, Lambers H, Cawthray GR, Pang J (2012) Carbon trading for phosphorus gain: the balance between rhizosphere carboxylates and arbuscular mycorrhizal symbiosis in plant phosphorus acquisition. *Plant Cell Environ* 35:2170–2180. <https://doi.org/10.1111/j.13653040.2012.02547.x>
34. Spohn M, Zavišić A, Nassal P, Bergkemper F, Schulz S, Marhan S, Schloter M, Schloter M, Kandeler E, Kandeler E, Polle A, Polle A (2018) Temporal variations of phosphorus uptake by soil microbial biomass and young beech trees in two forest soils with contrasting phosphorus stocks. *Soil Biol Biochem* 117:191–202. <http://doi.org/10.1016/j.soilbio.2017.10.019>
35. Sui WK, Li J, Wu XG, Wu QiY, Ma YM, Zhang XY, Zhang XJ (2020) Microbial mechanism of sulfide inhibiting N<sub>2</sub>O reduction during denitrification in fluvo-aquic soil. *Microbiol China* 47(10):3114–3125. <http://doi.org/10.13344/j.microbiol.china.200363>
36. Sun R, Li W, Hu C, Liu B (2019) Long-term urea fertilization alters the composition and increases the abundance of soil ureolytic bacterial communities in an upland soil. *FEMS Microbiol Ecol* 95:fiz044. <http://doi.org/10.1093/femsec/fiz044>
37. Tanaka M (2016) Recent progress in molecular studies on storage root formation in sweet potato (*Ipomoea batatas*). *Jarq-Jpn Agr Res Q* 50(4):293–299. <http://doi.org/10.6090/jarq.50.293>
38. Thomas RL, Sheard RW, Moyer JR (1967) Comparison of conventional and automated procedures for nitrogen, phosphorus, and potassium analysis of plant material using a single digestion. *Agron J* 59:240–243. <http://doi.org/10.2134/agronj1967.00021962005900030010x>
39. Villordon A, Gregorie JC, Labonte D (2020) Variation in phosphorus availability, root architecture attributes, and onset of storage root formation among sweetpotato cultivars. *HortScience: a publication of the American Society for Horticultural Science* 55(12):1903–1911. <http://doi.org/10.21273/HORTSCI15358-20>
40. Voges MJ, Bai Y, Schulze-Lefert P, Sattely ES (2019) Plant-derived coumarins shape the composition of an *Arabidopsis* synthetic root microbiome. *Proc Natl Acad Sci USA* 116:12558–12565. <http://doi.org/10.1101/485581>
41. Wang Y, Marschner P, Zhang F (2012) Phosphorus pools and other soil properties in the rhizosphere of wheat and legumes growing in three soils in monoculture or as a mixture of wheat and legume. *Plant Soil* 354(1–2):283–298. <http://doi.org/10.1007/s11104-011-1065-7>

42. Wang F, Shi N, Jiang R, Zhang F, Feng G (2016) In situ stable isotope probing of phosphate-solubilizing bacteria in the hyphosphere. *J Exp Bot* 67:1689–1701.  
<http://doi.org/10.1093/jxb/erv561>
43. Xiao W, Chen X, Jing X, Zhu B (2018) A meta-analysis of soil extracellular enzyme activities in response to global change. *Soil Biol Biochem* 123:21–32.  
<http://doi.org/10.1016/j.soilbio.2018.05.001>
44. Yu P, He X, Baer M, Beirinckx S, Hochholdinger F (2021) Plant flavones enrich rhizosphere Oxalobacteraceae to improve maize performance under nitrogen deprivation. *Nat Plants* 7:481–489.  
<https://doi.org/10.1038/s41477-021-00897-y>
45. Zhang L, Feng G, Declerck S (2018) Signal beyond nutrient, fructose, exuded by an arbuscular mycorrhizal fungus triggers phytate mineralization by a phosphate solubilizing bacterium. *ISME J* 12(10):2339–2351. <http://doi.org/10.1038/s41396-018-0171-4>
46. Zhalnina K, Louie KB, Zhao H, Mansoori N, da Rocha UN, Shi S, Cho H, Karaoz U, Loqué D, Bowen BP, Firestone MK, Northen TR, Brodie EL (2018) Dynamic root exudate chemistry and microbial substrate preferences drive patterns in rhizosphere microbial community assembly. *Nat Microbiol* 3:470–480. <https://doi.org/10.1038/s41564-018-0129-3>
47. Zheng L, Krishnamoorthi R, Zolkiewski M, Wang X (2000) Distinct Ca<sup>2+</sup>-binding properties of novel C2 domains of plant phospholipase D $\alpha$  and  $\beta$ . *J Bio Chem* 275:19700–19706.  
<http://doi.org/10.1074/jbc.M001945200>
48. Zhu XY, Zhao XR, Lin QM, Wang AL, Liu H, Wei HL, Sun WX, Li XC, Li YT GT (2020) Distribution characteristics of soil organic phosphorus fractions in the Inner Mongolia steppe. *J Soil Sci Plant Nutr* 12:2394–2405. <https://doi.org/10.1007/s42729-020-00305-y>
49. Zhu XY, Zhao XR, Lin QM, Li GT (2021) Distribution characteristics of *phoD*-harbouring bacterial community structure and its roles in phosphorus transformation in steppe soils in northern China. *J Soil Sci Plant Nutr* 21:1531–1541. <http://doi.org/10.1007/s42729-021-00459-3>

## Figures

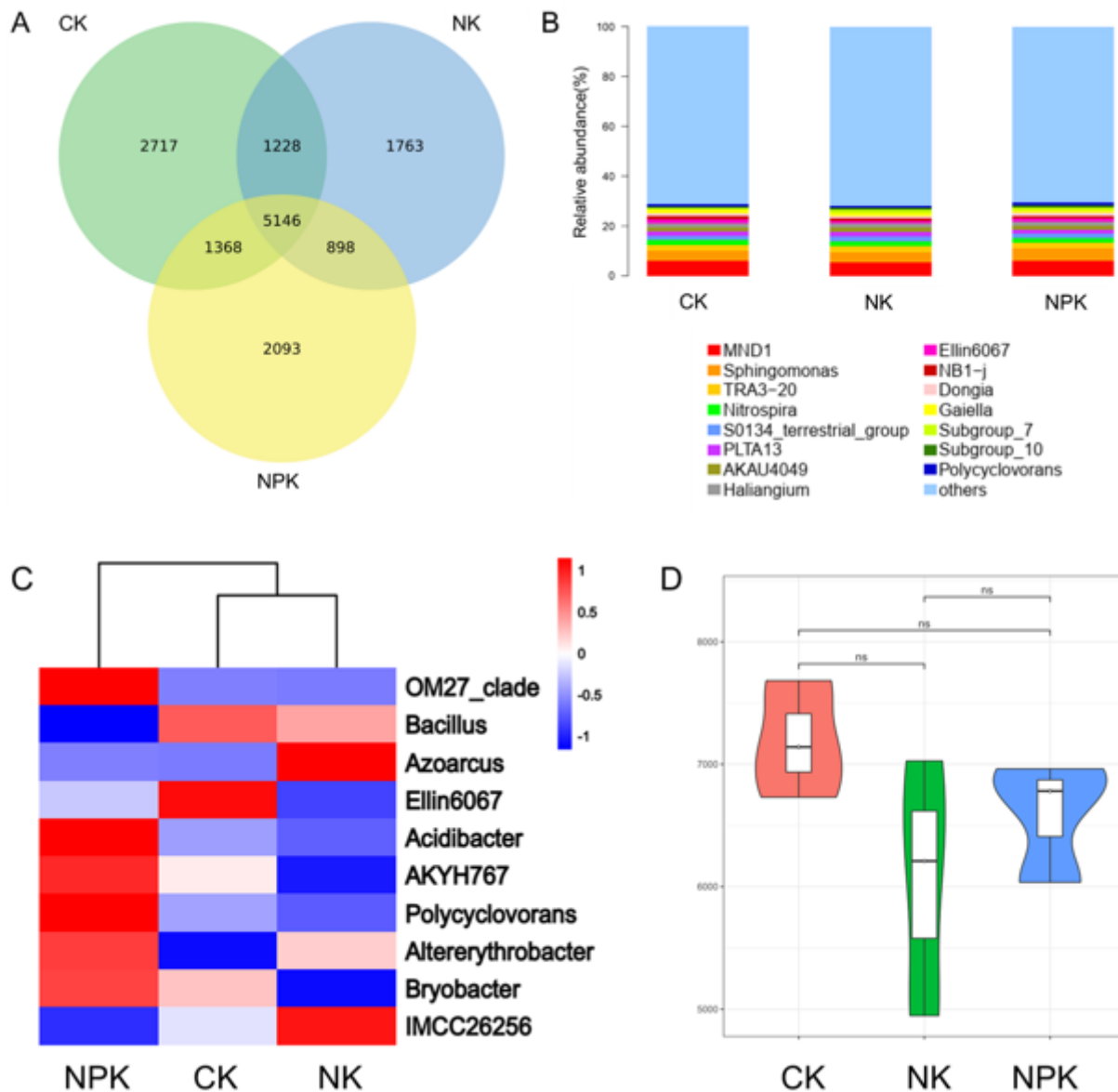


**Figure 1**

Venn diagram of unique and shared bacterial OTUs (A), top 15 dominant genera (B), top 10 differential genus (C) and  $\alpha$ -diversity of bacterial community Shangshu 19 rhizosphere among different treatments (D). Note: CK, NK and NPK represent non fertilization treatment, nitrogen and potassium application treatment and nitrogen, phosphorus and potassium application treatment, respectively. Same below

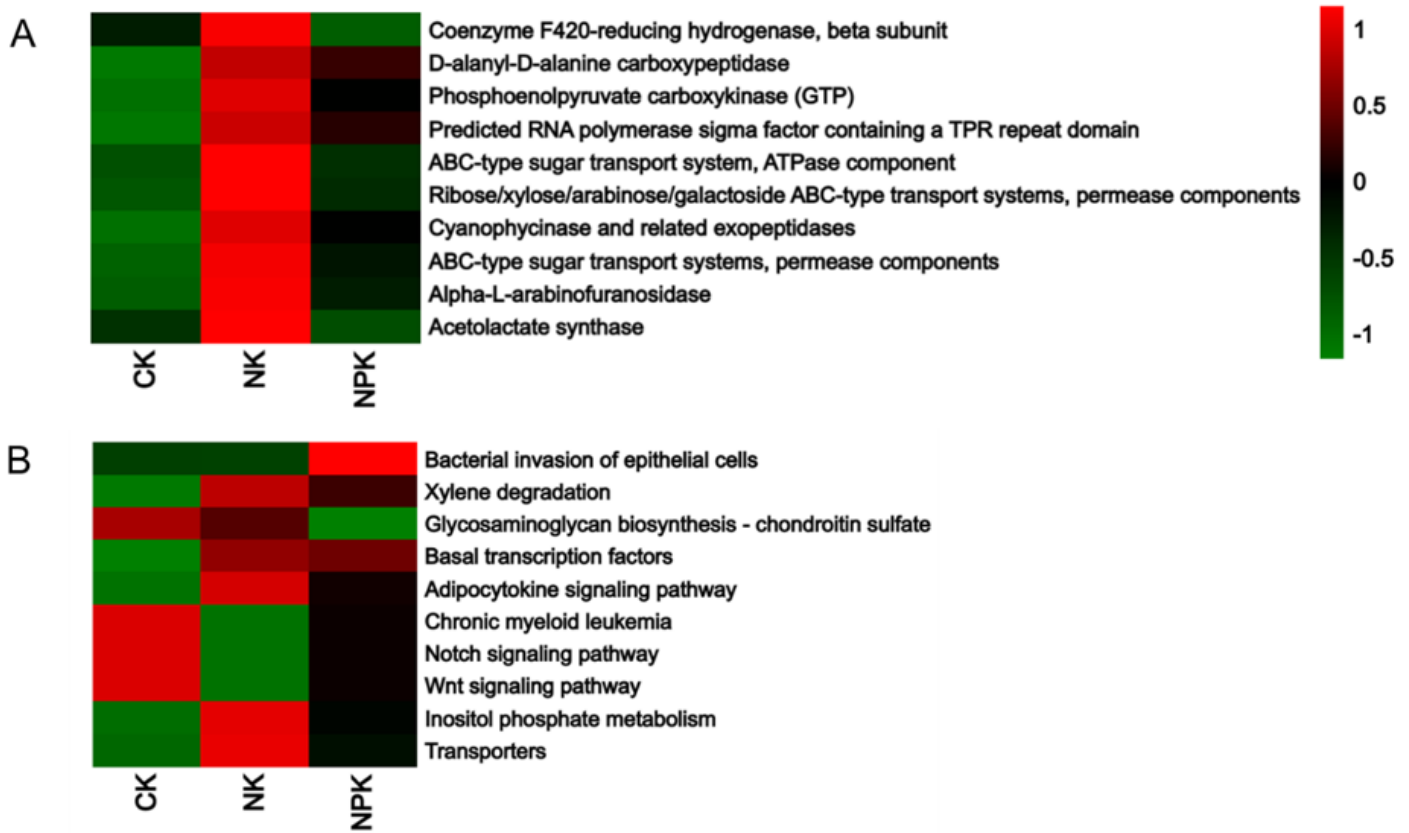


**Figure 2**

Prediction results of COG (top 10,  $P < 0.05$ ) (A) and KEGG\_L3 ( $P < 0.05$ ) (B) functions based on 16S rRNA sequences

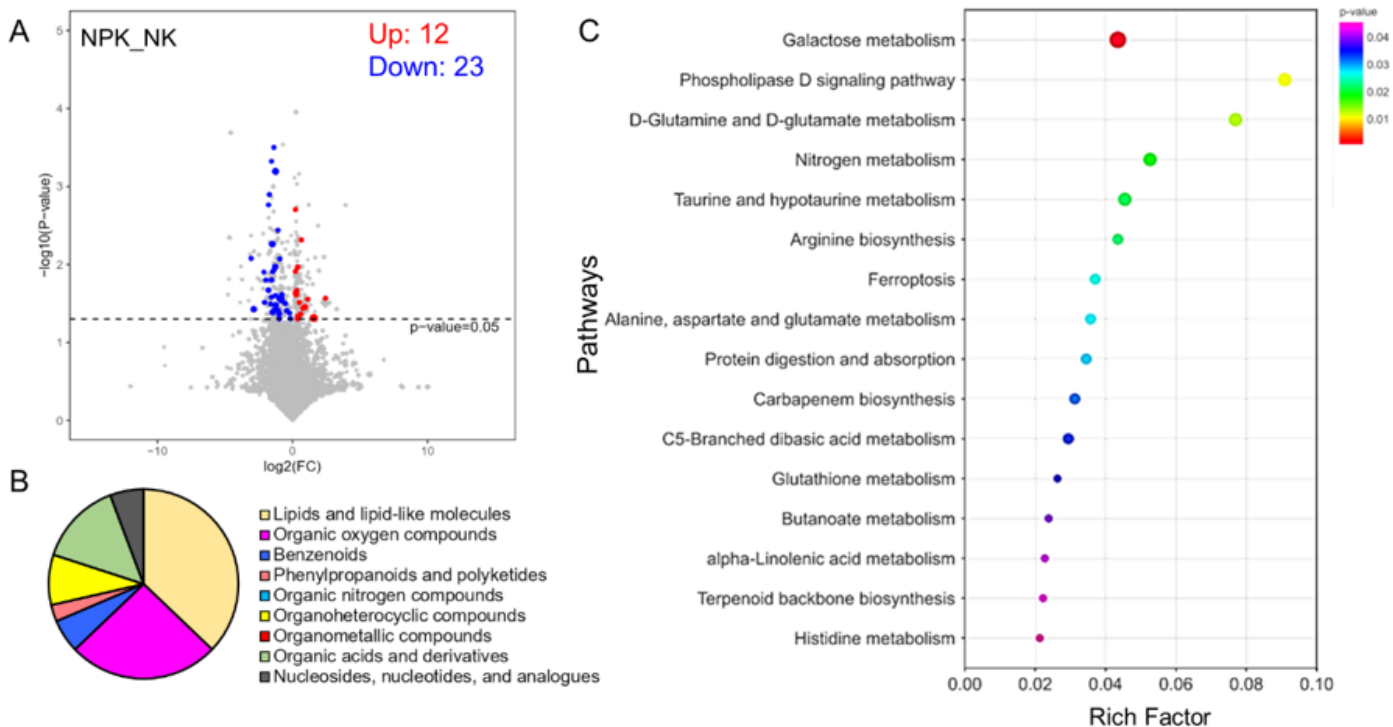


Figure 3

Volcano diagram of differentially expressed metabolites (DEMs) (A) and its taxonomy (B), KEGG enriched differential metabolic pathways (C) of Shangshu 19 rhizosphere

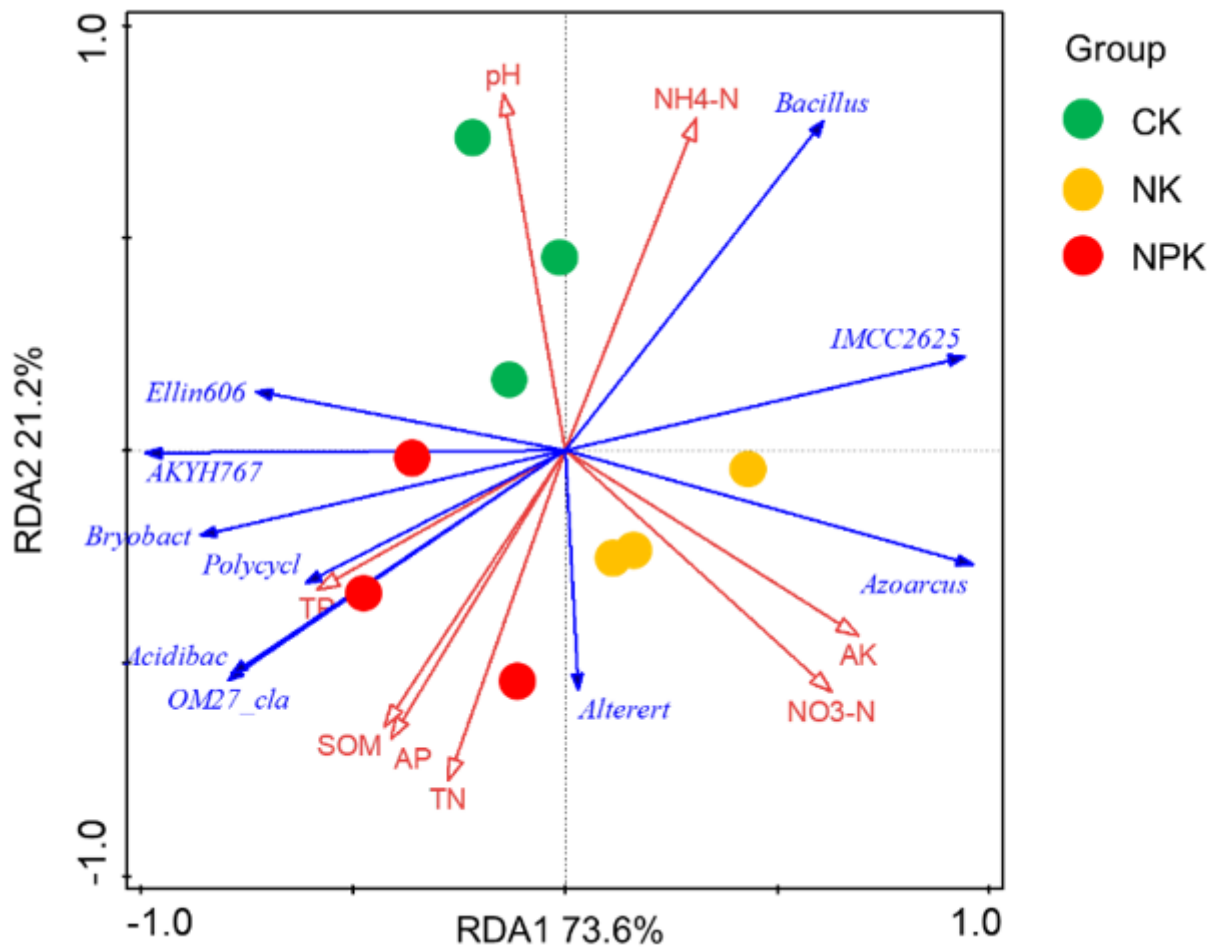


Figure 4

The effects of soil properties on bacterial community structure of Shangshu 19 rhizosphere

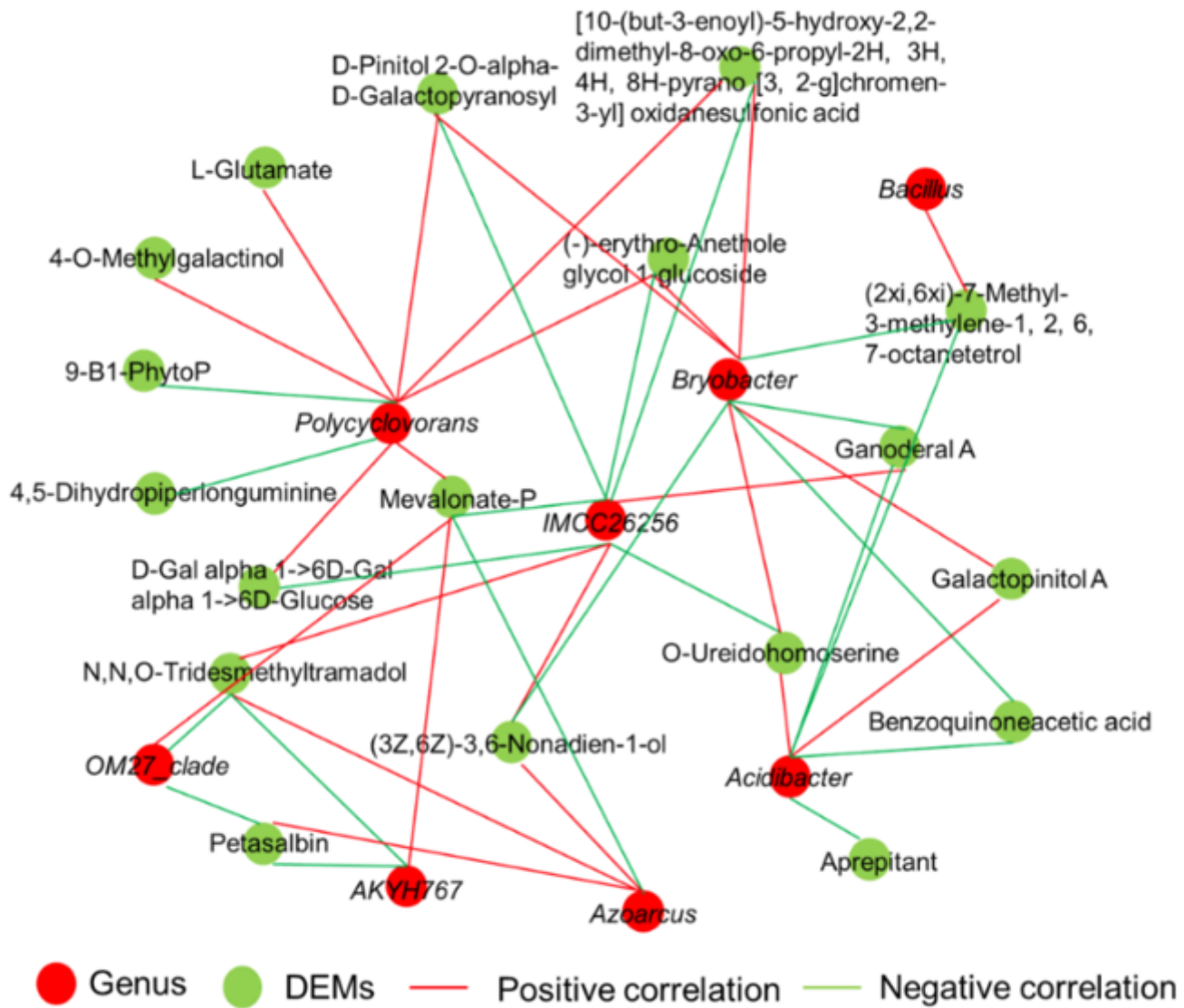


Figure 5

Networks analysis of differential genus with DEMs of Shangshu 19 rhizosphere

## Supplementary Files

This is a list of supplementary files associated with this preprint. Click to download.

- [Supplementaryinformations.docx](#)